High-pressure optical studies of doped alkali halides. I. Peak shifts and peak shape changes*

W. D. Drotning and H. G. Drickamer
Department of Physics, School of Chemical Sciences and Materials Research Laboratory, University of Illinois, Urbana, Illinois 61801
(Received 24 September 1975)

An apparatus has been developed which permits optical emission measurements to 150 kbar using a quasihydrostatic medium or to 12 kbar using a hydrostatic medium. Using this apparatus and the absorption rig already available, a series of high-pressure studies have been made on alkali-halide crystals doped with Tl^+ or In^+. In this paper we present data on the peak shifts and changes of shape and bandwidth. The following papers discuss Jahn-Teller effects, photothermally induced electron transfer, and mixed crystals. We discuss the shifts and shape changes in terms of a simple configuration coordinate model showing its possibilities and limitations. In spite of the fact that these systems are clearly too complex for such a simple description, one observes certain regularities. For several systems the decrease in volume upon electronic excitation is $\sim 10\%$ of the molecular volume. The ratio of force constants R of the excited state compared with the ground state is less than one. We demonstrate that several different methods for calculating R give consistent results.

A series of studies have been made on the effect of pressure on the optical absorption and emission spectra of heavy-metal-doped alkali halides. The optical-absorption apparatus has been previously described.[1,2] The emission cells are the same as the absorption cells, but with a window at 90° from the inlet. The pressure calibration utilizes the ruby fluorescence standard developed at the National Bureau of Standards[3]—the shift is -0.76–$0.77\ cm^{-1}/k$. Since the emission apparatus, operation, and data processing have not been previously described, some detail is given here. In most of these studies measurements have also been made to 10–12 kbars in a cell[4] using hexane as a truly hydrostatic-pressure fluid to test the effect of the quasihydrostatic medium (NaCl) used at high pressures. Except as indicated in paper III of this series, the hydrostatic results were identical with the quasihydrostatic data. This is consistent with the results of Okamoto and Drickamer[5] on organic samples.

The samples were made from Harshaw single-crystal alkali halides and reagent-grade monovalent dopants. (Chlorides were used for doping alkali chlorides and bromides; iodides for doping alkali iodides.) The materials were weighed into quartz tubes, sealed under vacuum, melted in a furnace, and cooled slowly. The concentration in the original sample was typically 0.01%. Optical-absorption measurements and, in a few cases, chemical analyses, indicated that the actual concentration in the crystal was a factor of 2–3 less than this. Doped crystals for several systems obtained from P. Yuster of Argonne Laboratory did not differ in behavior from those made in our laboratory.

EMISSION APPARATUS

Emission spectra can be recorded from 250 nm in the near uv through the visible spectrum to 1500 nm in the near ir. The spectrometer can also be employed to measure excitation spectra in the range 230–700 nm. A block diagram of the emission spectrometer apparatus is shown in Fig. 1.

The excitation light source is mounted in an LH 150 lamp housing, built by Schoeffel Instrument Corp. Lamps are powered by a Schoeffel LPS 271 power supply. For high-intensity excitation, an Osram HBO 200 W/2 200-W mercury arc lamp is used. For a somewhat weaker but broadband spectrum, a Hanovia 901C 150-W xenon arc lamp may be used. Under some circumstances a 200-W Hg-Xe lamp is also employed.

The exciting light is dispersed through two model 82-410 Jarrell-Ash quarter-meter Ebert monochromators, each equipped with two gratings. A quartz plano-convex lens then focuses the excitation light into the high-pressure cell.

The emitted light is observed at a right angle to the excitation light. A filter holder is positioned in the emission beam to allow rejection of reflected incident light from the sample, using a variety of filters. A quartz lens then collects the emitted light from the sample and focuses it onto the entrance slit of the emission monochromator, a Bausch and Lomb 500-mm grating monochromator. For emission in the near-uv and high-energy visible ranges, a grating blazed at 300 nm is used. For visible emissions, more light is transmitted using a grating blazed at 500 nm. The exit slit is variable; typically a 2-mm slit is used to allow a bandpass of 3.2 nm with the uv grating, and 6.6 nm with the visible grating. Several mercury lines are used to calibrate the monochromator.

For detection of the emitted light in the near uv and visible, the photomultiplier tube used is an EMI 9558 Q(A), cooled to −70° C, which is operated at a cathode voltage of −1200 V. This tube has a Spectrosil window for enhanced detection in the uv

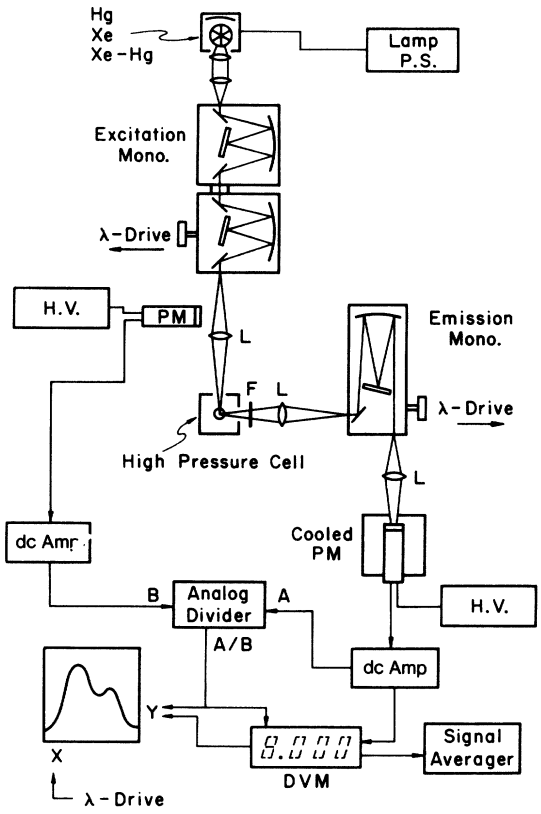

FIG. 1. Schematic diagram of high-pressure emission apparatus.

and employs a trialkali cathode with an S-20 response. Infrared tubes are available for long-wavelength radiation.

The dc amplified signal is displayed on a Dana model 4800 ratio digital voltmeter (DVM). The signal may also be displayed along the Y axis of a Hewlett-Packard model 7035B X-Y recorder. For particularly noisy signals, the measurement uncertainty may be reduced by signal-averaging techniques.

A small portion of the exciting light is reflected by the quartz lens in front of the high-pressure cell and is detected by an EMI 9529B photomultiplier tube aligned perpendicular to and out of the path of the exciting light. In this way compensation is made for variations in intensity of the lamp source and the nonuniform transmission of the excitation monochromator as functions of wavelength.

The apparatus used to measure excitation spectra is identical to the emission apparatus, described above, since the excitation technique employs essentially a measurement of emitted light. Often, both excitation and emission spectra are recorded on the same sample without removing the high-pressure cell from the apparatus. The EMI 9529B phototube is used to detect scattered incident light and thereby measure the flux of the excitation beam. For excitation spectra, the broad spectrum of the xenon arc lamp is required. A variable voltage source drives the X axis of an X-Y recorder; this source employs a constant voltage source and a 10-turn precision Helipot mechanically connected to the wavelength drive of the dual excitation monochromator.

Excitation spectra were compared to absorption spectra in materials (e.g., KCl:Tl) for which both spectra were obtained. No significant differences in band locations or shifts of bands with pressure were observed. Half-widths obtained from excitation spectra were on the order of 30% larger than absorption-spectra half-widths. This is most likely due to saturation effects which can yield flat-topped excitation peaks; however, the changes of these half-widths with pressure were found to reflect qualitatively similar changes in absorption-peak half-widths.

The fluorescence spectrum obtained directly from the emission spectrometer is not, in general, in a form suitable for analysis. First, the dynamic response of the emission measurement system is not independent of wavelength, so that a correction must be made for attenuation due to instrument response. Second, one frequently wants spectra which display relative emission as a function of photon energy, the relevant theoretical variable, instead of wavelength, the experimental independent variable. All emission spectra reported here have been corrected for these two factors.

Of the several methods reported for correcting for instrument response,[6-8] we used the standard lamp correction, following the treatment of Parker.[6]

The standard lamp used was a current-regulated tungsten-filament lamp with a quartz window and a spectral distribution calibrated against standards at the National Bureau of Standards. The response $R_{SL}(\lambda)$ of the system to this standard lamp was recorded for a number of combinations of photomultiplier tubes and monochromator gratings.

If $A(\lambda)$ is the measured spectrum as a function of wavelength and $dQ/d\nu$ is the number of quanta emitted per unit time for an energy interval $d\nu$, then

$$\frac{dQ}{d\nu} = A(\lambda)\frac{(dE/d\lambda)_{SL}}{R_{SL}(\lambda)}\lambda^3 . \qquad (1)$$

One can measure $R_{SL}(\lambda)$ for a given equipment configuration, use the data for $(dE/d\lambda)_{SL}$ of the standard lamp, and obtain the true spectrum $dQ/d\nu$ from the measured spectrum $A(\lambda)$. The correction factor was programmed for use with data measured with several combinations of detector tubes and gratings.

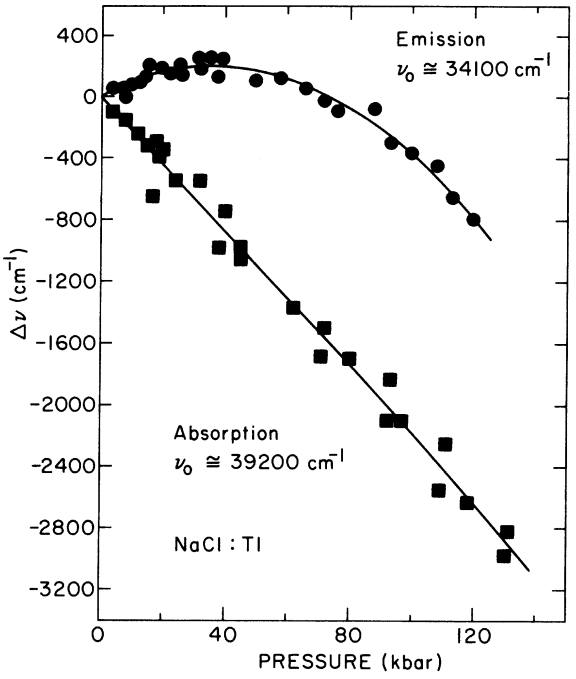

FIG. 2. Absorption and emission peak shifts vs pressure, NaCl : Tl.

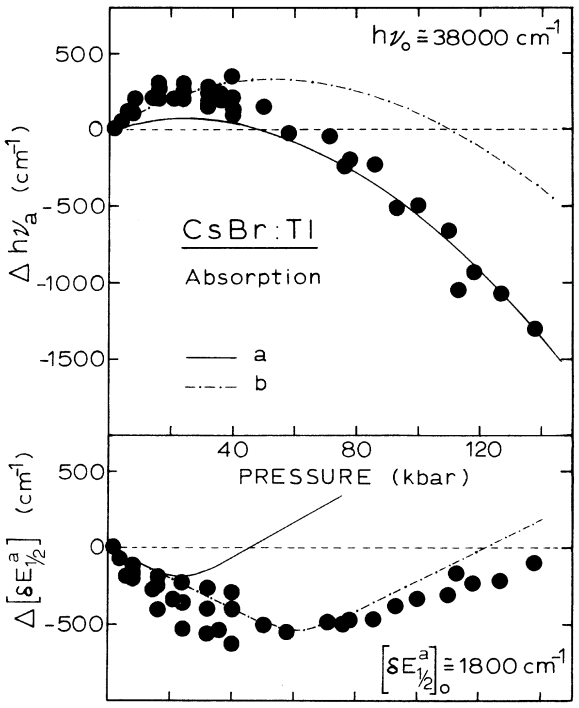

FIG. 4. Shift of absorption peak and change of half-width vs pressure, CsBr : Tl. The solid curves are calculated from peak-shift data; the dashed curves are calculated from half-width change data.

Corrections for spectral slit width and for sample self-absorption, as well as methods of fitting skewed peaks, are discussed elsewhere.[9,10]

RESULTS

There have been some high-pressure studies of the phosphors,[11–17] mostly in the range below 30 kbars, with very few attempts at analysis. In general, our results are consistent with the previous work where they overlap, when correction for revision of pressure scales is made.

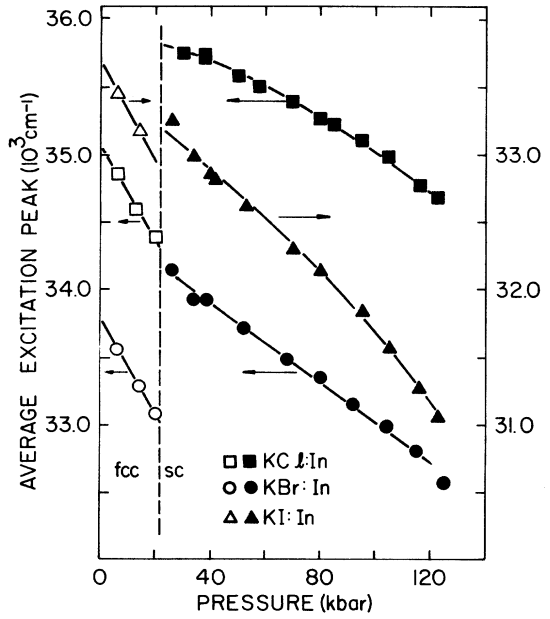

FIG. 3. Shift of excitation peak vs pressure, KCl : In, KBr : In, and KI : In in fcc and sc phases.

The effects of high pressure (quasihydrostatic to 140 kbars and hydrostatic to 10 kbars) on the emission and absorption properties of doped alkali-halide phosphors are presented. The results given here essentially involve the pressure-induced changes of band locations and half-widths.

Figures 2–6 exhibit data for representative systems which show the major features as well as typical scatter. Smoothed data appear in Tables I–IV. In the NaCl (fcc) phase the absorption peaks shifted to lower energy with increasing pressure and broadened slightly [(10–20)% in 100 kbars]. The emission peaks usually shifted slightly to higher energy at low pressure, exhibited a shallow maximum, and then a red shift at higher pressures. The half-widths decreased by (20–30)% in 100 kbars.

The potassium halides transform from the NaCl (fcc) structure to the CaCl (sc) phase at 18–19 kbars. Both absorption and emission peaks show discontinuities in energy at the transition.

In the sc phase the absorption peaks shifted to lower energy and decreased slightly in half-width.

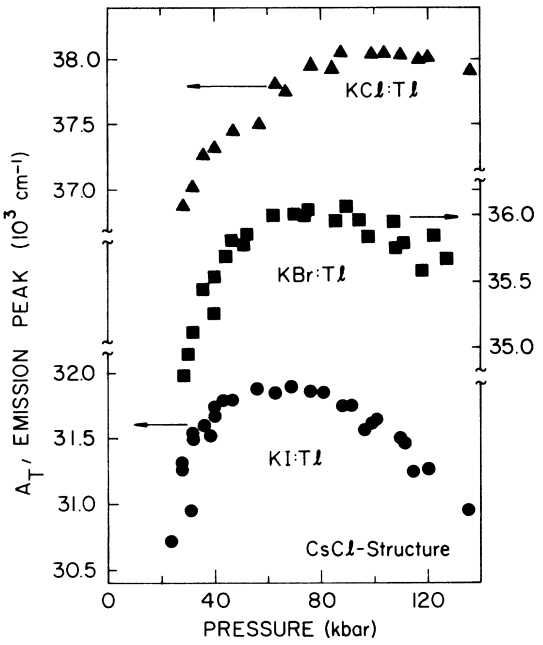

FIG. 5. Shift of $A_{T'}$ emission peak vs pressure, KCl : Tl, KBr : Tl, and KI : Tl in sc phase.

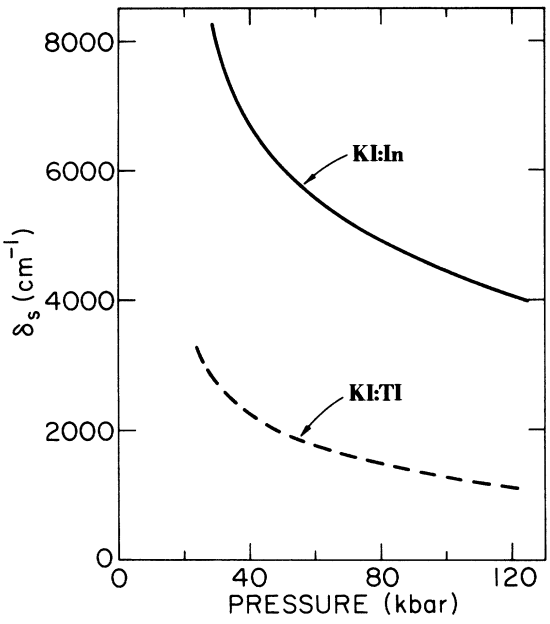

FIG. 7. Change of stokes shift vs pressure, KI : Tl and KI : In.

The absorption peaks for CsBr : Tl and CsI : Tl exhibited a small blue shift at low pressure and modest half-width increases. At higher pressure the peaks shifted to lower energy and broadened slightly. The emission peaks in the sc phase showed very strong shifts to higher energy at lower pressures, then maxima and small red shifts. Perhaps the most striking feature is the large decrease in half-width (by a factor of 2 or 3—see Fig. 6). This was accompanied by increasing distortion of the peak. Since the Stokes shifts decrease rapidly with pressure (see Fig. 7), one might attribute these changes in part to self-absorption. However, changes in sample size, shape, and geometry in the cell indicated that self-absorption was a negligible factor here.

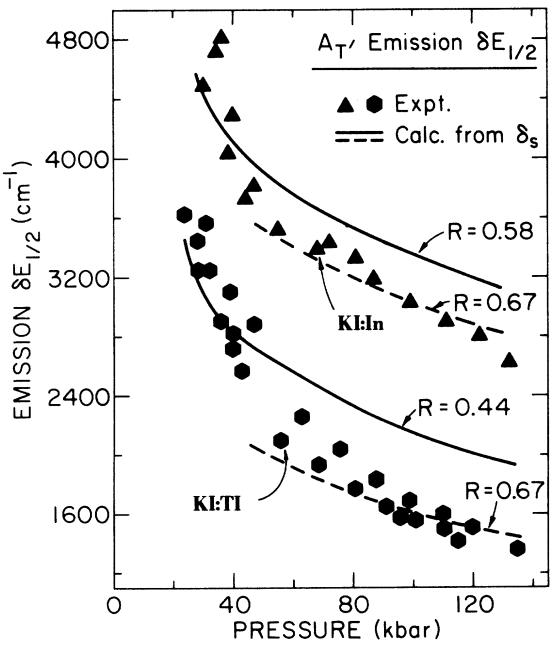

FIG. 6. Change of half-width vs pressure, KI : In and KI : Tl in the sc phase.

DISCUSSION

In this section we discuss the peak shifts and half-width changes in terms of parameters defined by a simple single-configuration-coordinate model. It is clear that the systems studied here are more complex than this model. The state to which the electron is excited in absorption is not, in general, the same electronic state as that from which emission occurs. It does not appear that for either of these processes individually only one configuration coordinate couples significantly to the pressure. Nevertheless, a discussion of such complex systems in simple terms sometimes reveals useful regularities.

As has been discusses in detail elsewhere,[9,18] for a localized excitation, one can describe the changes in peak location and half-width (assuming Gaussian peaks) by equations involving three parameters: q_0, the relative displacement of the potential wells along the configuration coordinate of interest at zero pressure, and ω^2 and $(\omega')^2$, the force constants for the ground and excited states. It is usually

TABLE I. Emission peak positions vs pressure. Locations in 10^3 cm^{-1}. The subscripts refer to Jahn-Teller–split components; the primes to the CsCl phase (see the following paper).

		Pressure (kbars)										
Compound		0	5	10	20	30	40	60	80	100	120	130
NaCl : Tl	A_T	34.10		34.18	34.26	34.28	34.30	34.20	34.02	33.73	33.30	
NaBr : Tl	A_T	32.30		32.52	32.60	32.66	32.65	32.46	32.13	31.73	31.22	
NaI : Tl	A_X	23.6		24.80	25.75	26.40	26.70	26.90	26.70	26.40	25.90	
	A_T	29.30		29.80	30.00	29.90	29.80	29.45	28.95	28.35	27.70	
NaCl : Ga	A_X	20.00		19.20	18.70	18.30	18.20	18.20	18.30	18.30	18.30	
	A_T	24.30		24.65	24.70	24.60	24.50	24.30	24.10	23.60	22.75	
KCl : Tl	A_T	32.80	32.98	33.12	33.22							
	$A_{T'}$					36.96	37.32	37.74	37.96	38.03	38.00	37.95
KBr : Tl	A_X	27.05	27.90	28.10								
	A_T	31.65	32.02	32.15	32.30							
	$A_{T'}$					35.00	35.50	35.92	36.20	35.92	35.73	35.60
KI : Tl	A_X	23.85	24.10	24.40	25.24							
	A_T	28.15	28.70	29.05	29.38							
	$A_{T'}$					31.40	31.70	31.86	31.85	31.62	31.26	31.02
KCl : In	A_T	23.35	23.35	23.35	23.35							
	$A_{T'}$					27.39	27.80	28.25	28.55	28.70	28.80	28.85
KBr : In	A_T	23.15	23.15	23.15	23.15							
	$A_{T'}$					25.90	26.65	27.15	27.45	27.60	27.60	27.55
KI : In	A_X	16.95	17.25	17.57	18.17							
	A_T	21.10	21.55	21.75	21.72							
	$A_{X'}$					18.30	19.45	21.10				
	$A_{T'}$					23.10	24.25	24.80	25.05	25.20	25.15	25.10
RbI : Tl	$A_{T'}$			30.80	31.65	32.20	32.38	32.40	32.27	32.00	31.60	
CsBr : Tl	$A_{X'}$	27.60	29.00	30.40	32.30	33.70						
	$A_{T'}$				34.40	35.05	35.48	35.85	35.88	35.72	35.38	
CsBr : In	$A_{X'}$	19.10	···	19.80	20.70	21.70	22.60	24.50				
	$A_{T'}$						25.20	26.40	27.10	27.30	27.20	27.10
CsI : In	$A_{X'}$	17.60	···	18.30	19.00	19.80	20.60	21.40	22.20	23.10		
	$A_{T'}$							24.50	25.20	25.40	25.20	25.20

more convenient to use ω^2 and $R=(\omega'/\omega)^2$. The relations obtained are

$$\Delta h\nu_a = pRq_0 + (R-1)p^2/2\omega^2 + \tfrac{1}{2}Rq_0^2(\omega^2-\omega_0^2)\ , \quad (2)$$

$$\Delta h\nu_e = pq_0/R + (R-1)p^2/2R^2\omega^2 - \tfrac{1}{2}q_0^2(\omega^2-\omega_0^2)\ , \quad (3)$$

$$(\delta E_{1/2})_a = N|\,\omega Rq_0 + p(R-1)/\omega|\ , \quad (4)$$

$$(\delta E_{1/2})_e = N|\,\omega q_0/R^{1/2} + p(R-1)/\omega R^{3/2}|\ , \quad (5)$$

where $N=(8kT\ln 2)^{1/2}$ for Gaussian peaks and $\omega_0=\omega$ at zero pressure. The relative displacement of the potential wells along the configuration coordinate $q(p)$ at any pressure (p) is

$$q(p) = q_0 + P(R-1)/\omega^2 R\ . \quad (6)$$

ω^2 and R may, in general, be functions of pressure. One might expect ω^2 to bear some relation to the

TABLE II. Emission peak half-widths vs pressure half-widths in 10^3 cm^{-1}. The subscripts refer to Jahn-Teller–split components; the primes to the CsCl phase (see the following paper).

		Pressure (kbars)										
Compound		0	5	10	20	30	40	60	80	100	120	130
NaCl : Tl	A_T	4.2		4.08	3.94	3.82	3.70	3.48	3.30	3.13	3.00	
NaBr : Tl	A_T	4.1		3.86	3.58	3.40	3.23	2.96	2.75	2.60	2.53	
NaI : Tl	A_T	6.0										
	A_X	4.0										
KCl : Tl	A_T	4.5	4.3	4.16	4.24							
	$A_{T'}$					4.00	3.54	3.00	2.70	2.45	2.25	2.16
KBr : Tl	$A_{T'}$					3.89	3.33	2.70	2.30	2.04	1.83	1.75
KI : Tl	$A_{T'}$					3.30	2.83	2.23	1.85	1.60	1.45	1.38
RbI : Tl	$A_{T'}$				3.20	2.55	2.10	1.66	1.46	1.36	1.33	1.32
CsBr : Tl	$A_{T'}$				3.60	3.20	3.00	2.65	2.35	2.15	2.08	2.00

TABLE III. Absorption peak location vs pressure. Locations in 10^3 cm^{-1}. The subscripts refer to Jahn-Teller-split components (see following paper).

		Pressure (kbars)										
Compound		0	10	20	30	40	60	80	100	120	130	140
NaCl: Tl		39.2		38.78		38.32	37.90	37.46	37.00	36.55		36.10
NaBr: Tl		37.40		36.88		36.44	36.00	35.52	35.04	34.76		34.27
NaI: Tl		34.00		33.56		33.15	32.70	32.23	31.73	31.20		30.68
KCl: Tl		40.20	39.95	39.75	40.90	40.86	40.70	40.48	40.26	40.00	39.86	
KBr: Tl		38.40	38.10	37.80	38.43	38.37	38.20	37.93	37.66	37.32	37.20	
KI: Tl		35.10	34.84	34.64	33.96	33.87	33.64	33.30	32.88	32.35	32.05	
KCl: In	A_1	34.35	34.00	33.65	35.15	35.08	34.87	34.62	34.33	34.06	33.90	
	A_2	35.72	35.42	35.12	36.38	36.35	36.20	36.00	35.75	35.43	35.25	
KBr: In	A_1	33.08	32.78	32.38	33.46	33.32	33.02	32.73	32.43	32.08	31.86	
	A_2	34.38	34.04	33.68	34.62	34.50	34.24	33.98	33.67	33.32	33.13	
KI: In	A_1	31.20	30.8	30.40	30.80	30.58	30.20	29.75	29.30	28.80		
	A_2	32.20	31.9	31.55	31.60	31.40	30.96	30.56	30.12	29.64		
RbI: Tl			34.10	34.07	34.03	33.96	33.76	33.45	33.02	32.52		
CsBr: Tl		38.00	38.16	38.25	38.25	38.20	38.04	37.80	37.47	37.05	36.80	
CsI: Tl		33.22	33.55	33.70	33.73	33.72	33.60	33.34	32.93	32.38		

bulk modulus of the lattice.

It is also possible to derive an expression for the Stokes shift observed in such a system in terms of R and the half-width of the emission peak,

$$\delta_S = [R(R+1)/2N^2]\,(\delta E_{1/2})_e^2. \tag{7}$$

One can also extract information about configuration-coordinate parameters from the asymmetry of the absorption or emission peak. There is considerable literature on this subject, which we need not discuss here.[19] In general, the asymmetry may be associated with a small value of q (the relative displacement along the configuration coordinate)—this is the so-called Huang-Rhys factor—or with quadratic electron-phonon coupling. Both factors may be present, but the analysis of most data in those terms becomes difficult. For our data it appears that the quadratic coupling factor is the dominant cause of asymmetry. We have discussed the methods of determining this in detail elsewhere[10] and only present here results which we use. It is possible to extract from the shape of the absorption or emission data a skewness factor b. By a series of numerical comparisons with the treatment of quadratic coupling by Jacobs and Thorsley,[20] one obtains a number of relations between b and the configuration coordinate parameters.

We shall use a relationship between the half-width, the skew parameter b, and R, all defined for

TABLE IV. Absorption peak half-widths vs pressure. Half-widths in 10^3 cm^{-1}. The subscripts refer to Jahn-Teller-split components (see following paper).

		Pressure (kbars)										
Compound		0	10	20	30	40	60	80	100	120	130	140
NaCl: Tl		1.80		1.80		1.86	1.91	1.98	2.03	2.10		2.16
NaBr: Tl		1.60		1.60		1.60	1.62	1.68	1.73	1.83		1.93
NaI: Tl		1.60		1.60		1.64	1.70	1.78	1.87	1.97		2.07
KCl: Tl		1.65	1.67	1.69	1.25	1.21	1.15	1.15	1.25	1.33	1.37	
KBr: Tl		1.36	1.40	1.46	1.15		1.15		1.16		1.16	
KI: Tl		1.25	1.25	1.25	1.25	1.23	1.10	1.06	1.05	1.06	1.08	
KCl: In	A_1	2.30	...	2.30	1.90						1.90	
	A_2	1.20		1.20	1.10						1.10	
KBr: In	A_1	2.10		2.10	1.80						1.80	
	A_2	1.10		1.10	1.10						1.10	
KI: In	A_1	2.0		2.0	1.7						1.7	
	A_2	1.0		1.0	0.9						0.9	
RbI: Tl			1.35	1.28	1.22	1.16	1.06	1.08	1.10	1.15		
CsBr: Tl		1.80	1.60	1.50	1.40	1.35	1.28	1.30	1.40	1.60	1.70	
CsI: Tl		1.45	1.32	1.21	1.15	1.09	0.99	0.99	0.91	0.95		

TABLE V. Configuration coordinate parameters determined from high-pressure model. Ω, molecular volume (of an anion-cation pair); ω^2 in units kbars^2/cm.

	Absorption			Emission		
System	R	ω^2	q_0/Ω	R	ω^2	q_0/Ω
NaCl : Tl	0.88	6.8	−0.11	0.60	3.6	0.027
NaBr : Tl	0.87	6.2	−0.09	0.45	7.3	0.020
NaI : Tl	0.58	6.2	−0.10	a	a	a

[a]Jahn-Teller interaction causes emission doublet.

the emission process:

$$b(\delta E_{1/2}) = (586\,\mathrm{cm}^{-1})\,(R-1)/R\ . \tag{8}$$

It has been previously demonstrated[5,21] that a single-configuration-coordinate model is adequate to describe peak shifts and half-width changes for aromatic molecules in various environments and that consistent values of the parameters can be extracted from absorption and emission data or from combinations of these. From the directions of the shifts of the absorption and emission peaks for the systems discussed here (as well as from half-width data), it is clear that the state to which an electron is excited in absorption is *not* the same as that from which emission occurs. This is in any case clear from the discussion of the Jahn-Teller effect in these crystals, which we treat elsewhere.

An examination of the absorption (or emission) shifts and half-width changes with pressure indicates that there is only qualitative agreement with the equations as presented, so that the single-configuration-coordinate model is only a first-order description of the absorption or emission process. There are available more complex analyses[22] involving more parameters. It does not appear that the data warrant the use of more parameters and, in any case, it does not appear that reasonable values of the parameters would account for all the discrepancies. The limitation appears to be the use of a single-configuration-coordinate model.

We have extracted values for the parameters q_0, R, and ω^2 from the absorption and emission data for Tl^+ in the sodium halides, assuming R and ω^2 do not depend on pressure. These appear in Table V. There is reasonable consistency for the different halides. The negative value for q_0/Ω indicates that there is a measurable volume decrease when an electron is excited. However, the state from which an electron is emitted in fluorescence is slightly larger than the ground state.

A similar calculation was attempted for CsBr : Tl. As can be seen from Fig. 4, the best quadratic fit to the shift data predicts qualitatively the features of the half-width (solid lines) change, and vice versa (dashed lines), but there is not quantitative agreement.

We turn now to the calculation of R from various aspects of data and show that, in fact, reasonably consistent values can be obtained both for the magnitude and pressure dependence.

Since the Stokes shift is related to the emission half-width by Eq. (7), one can solve for R vs pressure. The Stokes shift in two representative systems is shown in Fig. 7. All A_T, emissions yield similarly decreasing Stokes shifts. Using (7), one can compare the experimental half-widths to those calculated from the observed Stokes shift and a particular R. These calculations are shown in Fig. 6 for two different values of R which fit the half-width data in the low- and high-pressure regions, respectively. The agreement is quite good, considering that a single-configuration-coordinate model surely oversimplifies the situation. Only a slightly pressure-dependent R is necessary to give excellent agreement. Conversely, using the observed Stokes shifts δ_S and emission half-widths, one can calculate R vs pressure explicitly from (7). These results are given as method A in Table VI

TABLE VI. R vs pressure from $A_{T'}$ emission bands. Method A calculated from Stokes shift and $(\delta E_{1/2})_e$, using Eq. (7); method B calculated from skewness b and $(\delta E_{1/2})_e$, using Eq. (8); method C calculated from Eqs. (4) and (5), using $(\delta E_{1/2})_e$ and $(\delta E_{1/2})_{abs}$ (corrected for slit width).

	KCl : Tl			KBr : Tl		KI : Tl			RbI : Tl		KCl : In		KBr : In		KI : In	
P	A	B	C	A	B	A	B	C	A	B	A	B	A	B	A	B
25	0.39	0.30		0.38	0.32	0.37	0.28			0.37		0.43		0.48		
30	0.41	0.31	0.44	0.39	0.33	0.39	0.31	0.52	0.46	0.40	0.58	0.44	0.57	0.51	0.50	0.39
40	0.45	0.34	0.45	0.42	0.37	0.44	0.34	0.57	0.54	0.44	0.63	0.46	0.64	0.55	0.58	0.44
50	0.48	0.36	0.48	0.46	0.40	0.49	0.37	0.59	0.61	0.48	0.63	0.47	0.68	0.57	0.63	0.47
60	0.50	0.38	0.50	0.49	0.42	0.54	0.40	0.62	0.68	0.50	0.63	0.47	0.67	0.57	0.64	0.48
70	0.52	0.39	0.54	0.52	0.44	0.58	0.42	0.65	0.72	0.52	0.64	0.48	0.68	0.58	0.64	0.49
80	0.53	0.40	0.56	0.54	0.46	0.62	0.44	0.68	0.75	0.53	0.64	0.49	0.68	0.59	0.64	0.50
90	0.54	0.42	0.60	0.57	0.47	0.64	0.46	0.71	0.76	0.54	0.64	0.49	0.69	0.59	0.64	0.50
100	0.55	0.43	0.64	0.60	0.49	0.67	0.48	0.75	0.74	0.55	0.65	0.50	0.71	0.60	0.66	0.52
110	0.57	0.44	0.66	0.63	0.50	0.69	0.49	0.76	0.74	0.56	0.65	0.50	0.73	0.61	0.68	0.53
120	0.59	0.45	0.70	0.66	0.52	0.72	0.50	0.80	0.77	0.56	0.67	0.51	0.75	0.62	0.70	0.54
130	0.61	0.46	0.73	0.70	0.53	0.74	0.51	0.84								

TABLE VII. Skewness parameter b for A_T emission peaks, from computer fits. Values given represent an average b over the range 30–130 kbars, with the variance an indicator of the changes in this pressure range.

System	$-b$
KCl : Tl	0.32 ± 0.04
KBr : Tl	0.30 ± 0.05
KI : Tl	0.40 ∓ 0.05
Rb : Tl	0.35 ± 0.06
KCl : In	0.16 ± 0.1
KBr : In	0.12 ± 0.01
KI : In	0.18 ± 0.02

for the In^+- and Tl^+-doped potassium halides and RbI : Tl. In all cases, R is seen to increase with pressure.

Two additional methods may be used for calculating R. The observed asymmetry of the A_T band can be described by the fit values of the skewness b. Average values of b for the relevant materials are given in Table VII. From Eq. (8), values of b, and the emission half-widths $(\delta E_{1/2})_e$, one can solve for R. The results are given by method B in Table VI. Although differences exist between the values of R determined by methods A and B, the trends with pressure are similar: R increases with increasing pressure.

Assuming R is correctly determined by method A, one can calculate an expected skewness b. For example, for KCl : Tl at 50 kbars, $R = 0.48$ and $(\delta E_{1/2})_e = 3230\ \mathrm{cm}^{-1}$ yields $b = -0.20$. The measured value is $b = -0.32 \pm 0.04$. The minor discrepancy is further evidence that self-absorption effects are small.

Values of R may also be found from the ratio of $(\delta E_{1/2})_{abs}$ to $(\delta E_{1/2})_e$, which is $R^{3/2}$. Having corrected the bandwidths for the slit width, the values of R determined in this way are given in Table VI as method C. Again, R is observed to increase with pressure, and has a value of roughly 0.5–0.7. The agreement is quite good among the three methods of obtaining R.

*Supported in part by the U.S. ERDA under Contract E(11-1)-1198.

[1]R. A. Fitch, T. E. Slykhouse, and H. G. Drickamer, J. Opt. Soc. Am. 47, 1015 (1957).
[2]H. G. Drickamer and A. S. Balchan, in *Modern Very High Pressure Techniques*, edited by R. H. Wintorf, Jr. (Butterworths, London, 1962), p. 25.
[3]G. Piermarini, S. Block, J. D. Barnett, and R. A. Foreman, J. Appl. Phys. 46, 2774 (1975).
[4]G. Weber, R. Tanaka, B. Y. Okamoto, and H. G. Drickamer, Proc. Natl. Acad. Sci. USA 71, 1264 (1974).
[5]B. Y. Okamoto and H. G. Drickamer, J. Chem. Phys. 61, 2870 (1974).
[6]C. A. Parker and W. T. Rees, Analyst 85, 585 (1960).
[7]C. A. Parker, *Photoluminescence of Solutions* (Elsevier, New York, 1968).
[8]C. E. White and R. J. Argauer, *Fluorescence Analysis: A Practical Approach* (Dekker, New York, 1970), pp. 30–53.
[9]B. Y. Okamoto, W. D. Drotning, and H. G. Drickamer, Proc. Natl. Acad. Sci. 71, USA 2671 (1974).
[10]C. E. Tyner, W. D. Drotning, and H. G. Drickamer J. Appl. Phys. 47, 1044 (1976).
[11]R. A. Eppler and H. G. Drickamer, J. Phys. Chem. Solids 6, 180 (1958).
[12]R. A. Eppler and H. G. Drickamer, J. Phys. Chem. Solids 15, 112 (1960).
[13]A. I. Laisaar and Y. Y. Kirs, Bull. Acad. Sci. USSR Phys. Ser. 33, 917 (1969).
[14]P. B. Alers and R. L. Dolecek, J. Chem. Phys. 38, 1046 (1963).
[15]P. B. Alers and P. E. V. Shannon, J. Chem. Phys. 41, 1675 (1964).
[16]S. Masunaga and M. Ishiguro, J. Phys. Soc. Jpn. 25, 1337 (1968).
[17]P. D. Johnson and F. E. Williams, Phys. Rev. 95, 69 (1954).
[18]H. G. Drickamer, C. W. Frank, and C. P. Slichter, Proc. Natl. Acad. Sci. 69, 933 (1972).
[19]M. Stoneham, *Defects in Solids* (Oxford U.P., Oxford, England, 1975).
[20]P. W. M. Jacobs and S. A. Thorsley, Cryst. Lattice Defects 5, 51 (1974).
[21]B. Y. Okamoto and H. G. Drickamer, Proc. Natl. Acad. Sci. 71, 4757 (1974).
[22]C. S. Kelley, Phys. Rev. B 12, 594 (1975).